Department of Chemical Engineering
University of California, Santa Barbara

CH E 180B. Chemical Engineering Laboratory

Batch to Continuous Process Development: Kinetic and Mixing analysis of Saponification of Ethyl Acetate with Sodium Hydroxide in CSTR

Sean Shen, Yulun Wu, Chang Yuan
Group 9W

Experiment Conducted between January 15th and January 29th, 2025
Report Submitted on February 5th, 2025

1 Abstract

The transition from batch to continuous processing in chemical manufacturing enhances efficiency, scalability, and process control. This study examines viability of producing sodium acetate (NaAc) from ethyl acetate (EtAc) waste streams through saponification with sodium hydroxide (NaOH) from batch reactor to a Continuous Stirred Tank Reactor (CSTR). The second-order rate law was confirmed, yielding an activation energy $E_a = (33.0 \pm 1.2)$kJ/mol, and a pre-exponential factor $A = (3.8 \pm 0.3) \times 10^4 \text{s}^{-1}$, calculated using the Arrhenius equation. Following the kinetic analysis, the CSTR performance was assessed under varying flow rates ($Q = 100, 200, 300$ mL/min) with a mean residence time of ($259.1 \pm 5s$, $254.2 \pm 5s$, $219.1 \pm 5s$) respectively. Residence Time Distribution (RTD) analysis revealed back-mixing effects, particularly at lower flow rates, influencing conversion efficiency. The conversion exhibited a nonlinear dependence on residence time, with a maximum observed conversion of $33.51 \pm 0.15\%$ at $Q = 200$ mL/min. This study provides quantitative insights into the relationship between residence time, flow rate, and reaction kinetics, contributing to the optimization of continuous saponification processes. The findings guide reactor design and scale-up for efficient sodium acetate production while maintaining process control.

2 Introduction

The transition from batch to continuous processing in chemical manufacturing offers significant advantages in efficiency, scalability, and process control. In this study, we focus on the continuous production of sodium acetate (NaAc) from ethyl acetate (EtAc) waste streams through saponification with sodium hydroxide (NaOH), governed by the reaction[**2**]:

$$\text{NaOH} + \text{EtAc} \rightarrow \text{NaAc} + \text{EtOH} \tag{1}$$

This reaction follows a second-order rate law since it involves two reactants in a bimolecular reaction. The rate of reaction can be expressed as[**2**]:

$$r_A = -\frac{dC_A}{dt} = kC_AC_B \tag{2}$$

where C_A and C_B are the concentrations of NaOH and EtAc, respectively, and k is the second-order rate constant. The integrated form of the second-order rate equation for equal initial concentrations of both reactants ($C_A = C_B$) is given by[**2**]:

$$\frac{1}{C_A} - \frac{1}{C_{A0}} = kt \tag{3}$$

where C_{A0} is the initial concentration of reactant A, and t is the reaction time. The kinetic coefficient k can thus be determined from the slope of a plot of $\frac{1}{C_A}$ versus time.

we use a conductivity probe to monitor reactant conversion and determine concentration in real-time. The conductivity (Λ) of the solution is influenced primarily by the

presence of ionic species (NaOH and NaAc), allowing us to relate conductivity to NaOH concentration through the equation[**2**]:

$$[\text{NaOH}] = [\text{NaOH}]_0 \frac{\Lambda - \Lambda_\infty}{\Lambda_0 - \Lambda_\infty} \tag{4}$$

where Λ_0 and Λ_∞ are the initial and final conductivities corresponding to known concentrations.

To design an optimized reactor system, we must determine the reaction kinetics, which are influenced by temperature and reactant concentration. The temperature dependence of the reaction rate follows the Arrhenius equation[**2**]:

$$k = Ae^{-\frac{E_a}{RT}} \tag{5}$$

where k is the rate constant, A is the pre-exponential factor, E_a is the activation energy, R is the universal gas constant, and T is the absolute temperature.

For batch reactor studies, the concentration of reactants changes over time and is described by the batch reactor design equation[**5**]:

$$\frac{dC_A}{dt} = -r_A \tag{6}$$

Once the reaction kinetics are established, we extend our analysis to a continuous stirred-tank reactor (CSTR), described by the steady-state reactor design equation[**4**]:

$$C_{A0} - C_A + \tau R_A = 0 \tag{7}$$

where C_{A0} and C_A are the concentration of reactant A at the inlet and outlet, respectively, R_A is the reaction rate, and τ is the residence time.

To characterize the flow behavior within the CSTR, the residence time distribution (RTD) is determined using the step-change method. A NaCl tracer solution is introduced at a constant concentration, and the outlet concentration is monitored over time. The cumulative residence time distribution function, $F(t)$, is obtained from the measured concentration profile[**3**]:

$$F(t) = \frac{C_(t)}{C^(0)} \tag{8}$$

where $C^*(0)$ is the initial concentration and $C^(t)$ represents the outlet concentration correlated with time. The residence time distribution function, $E(t)$, is then obtained by differentiating $F(t)$[**3**]:

$$E(t) = \frac{dF(t)}{dt} \tag{9}$$

The mean residence time, t_m, is given by[**3**]:

$$\tau = \int_0^\infty tE(t)dt \tag{10}$$

which represents the average residence time τ of the CSTR.

By integrating these fundamental equations and experimental data, this study aims to characterize reaction kinetics, assess the impact of mixing and residence time on reactor performance, and provide recommendations for scaling up the process to industrial production.

3 Method

The reaction kinetics of sodium acetate formation via saponification of ethyl acetate with sodium hydroxide were determined using a batch reactor and a continuous stirred tank reactor (CSTR). The experimental setup, shown in Figure 1, consists of a stirred reaction vessel, a conductivity probe, peristaltic pumps, and a temperature-controlled water jacket. The batch reactor experiment was conducted at controlled temperatures in the range of $10.0 \pm 0.1\,^\circ$C to $40.0 \pm 0.1\,^\circ$C. The relationship between conductivity and concentration was determined using the conductivity probe by allowing an excess of ethyl acetate (EtAc) to fully react with sodium hydroxide (NaOH) until the reaction reached completion. The initial and final conductivity measurements were then used to establish a linear calibration curve, correlating conductivity with concentration.

The batch reactor experiments were performed to determine the reaction kinetics under controlled conditions. Equal volumes of 0.1M sodium hydroxide (NaOH) and 0.1M ethyl acetate (EtAc) were mixed at the same time in the test tube. The reaction mixture was maintained at constant temperature using a recirculating water bath. A conductivity probe continuously measured the conductivity of the solution over time, allowing for the determination of reaction progress. The experiment was repeated at different temperatures to observe the effect of temperature on reaction kinetics. The Arrhenius Equation is then applied to find out the pre-exponential factor and activation energy of the reaction.

Following the batch reactor experiments, a CSTR was used to analyze the reaction under continuous flow conditions. The peristaltic pumps controlled the inlet flow rates of NaOH amd EtAc, ensuring a consistent feed into the reactor. Prior to the experiment, the pumps were calibrated by measuring the volume of liquid delivered over time at different speed settings to establish a flow rate correlation. Figure 1 shows the apparatus of the CSTR system.

Residence time distribution (RTD) was evaluated by introducing a NaCl tracer pulse into the inlet and monitoring the change in conductivity over time at the outlet. By varying the mixing speed, the effect of mixing on RTD was investigated. The RTD curve provided insights into mixing efficiency and was used to determine the average residence time for the CSTR. Before conductivity measurements were taken at the outlet, the reactor was allowed to reach steady-state conditions. To ensure accuracy, the system was left undisturbed for a sufficient period. The calibration relationship established in the batch experiment was applied to determine the outlet concentration. Flow rates were adjusted between 100 and 300 mL/min to analyze the effect of residence time on reaction

conversion.

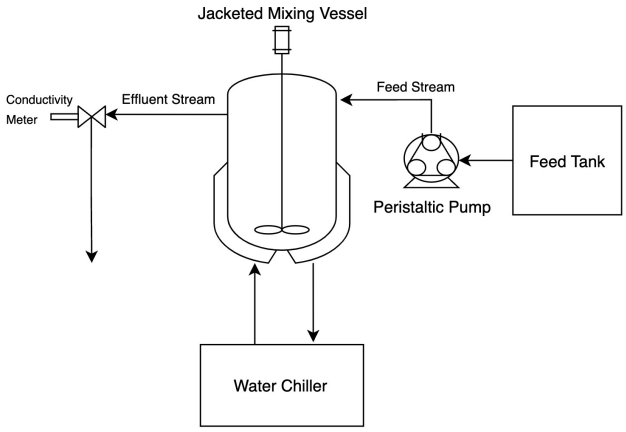

Figure 1: Schematic of the Continuous Stirred Tank Reactor (CSTR) System. The system consists of a jacketed mixing vessel with a controlled feed stream supplied by a peristaltic pump, drawing reactants from the feed tank. A water chiller maintains a stable reaction temperature. The reaction progress is monitored using a conductivity meter placed at the effluent stream outlet, allowing for real-time concentration measurements.

4 Results and Discussion

4.1 Determination of Reaction Coefficient, Pre-exponential Factor and Activation Energy using Batch-type Reactor

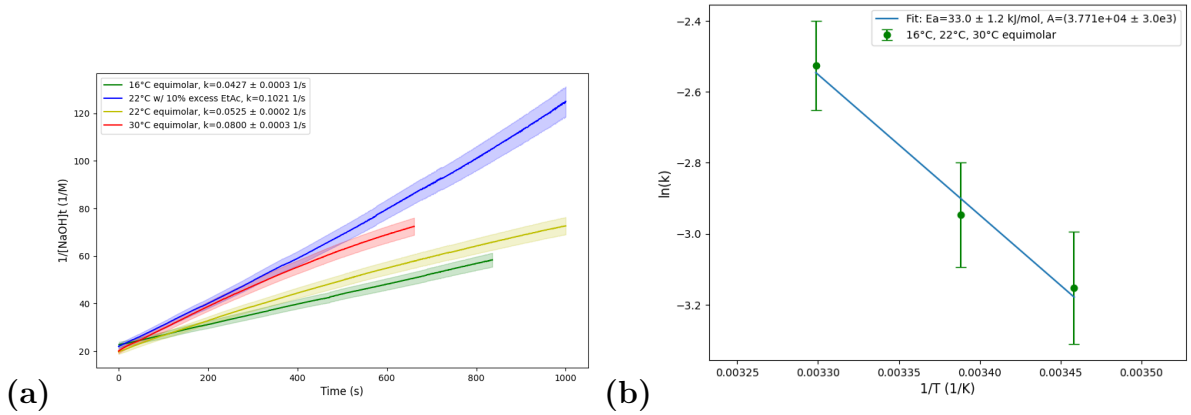

Figure 2: **(a)** Second Order Integrated Rate Equation Displaying: 1/[NaOH]t vs. Time for Saponification Reaction at Different Temperatures. The plot depicts the linear relationship of inverse NaOH concentration and time. The slope of the resulting straight lines indicate the reaction rate coefficients (k) at which the reaction takes place at 16°C, 22°C, and 30°C. (b) Arrhenius Plot of ln(k) vs. 1/T for the Saponification Reaction. This plot illustrates the temperature dependence of k for the saponification reaction. The linear fit follows the Arrhenius equation (Eqn.5) yielding an activation energy E_a and a pre-exponential factor A.

The saponification of EtAc by NaOH was studied in batch-type reactors by continuously measuring the electric conductivity of the reaction solution. Only NaOH and NaAc contribute to the conductivity, but the conductivity of NaOH at a given temperature and concentration is independent of other components in this case. This allows for proper measurement of [NaOH] in the reaction mixture. The second order kinetics plot (Fig.2a) of 1/[NaOH]t vs. time, showing a linear trend, confirms the assumed reaction order. The slopes of the fitted lines provide the reaction rate coefficients at the tested temperatures of 16°C, 22°C, and 30°C. In the case of the 22 ° C reaction with excess 10% EtAc, the determined k is significantly higher, suggesting interference of the effects of mass transfer on reaction speed. Thus, it is excluded from the linear regressing conducted in the latter calculation where the temperature dependence of k is determined. However, in other measurements, k increases with temperature, following an intuitive sense. Using the Arrhenius equation (Eqn.5), an activation energy equal to 33.0 kJ / mol and a pre-exponential factor equal to $3.8 * 10^4$ are approximated. The results have a 31% deviation from reported data [**1**]. As shown in raw data, temperature fluctuates around the set point, and a gradual decrease of temperature is observed. Inaccurate temperature measurements can affect Arrhenius analysis, leading to underestimation of E_a. A lower E_a suggests that the reaction can proceed more easily than reported, and therefore, when using parameters obtained from our measurements, estimated values of k increase more gradually with temperature. Additionally, it is notable that increase in viscosity leads to a decrease in reaction rate, primarily due to diffusion limitations – reacting species move more slowly in mediums that are more viscous [**2**].

4.2 Investigation of Mixing Speed Effects on Residence Time Distribution and Mean Residence Time

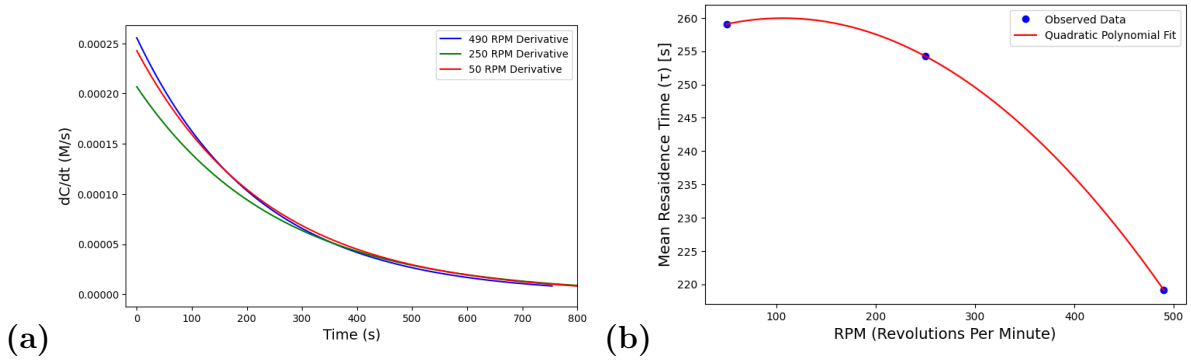

(a) **(b)**

Figure 3: **(a)** Residence Time Distribution (RTD) function for the CSTR at Various Mixing Speeds. This plot depicts the rate of concentration change ($\frac{dC}{dt}$) over time for the continuous stirred tank reactor (CSTR) at different impeller speeds: 50 RPM (red), 250 RPM (green), and 490 RPM (blue). (b) Relationship Between Mean Residence Time and Mixing Speed in the CSTR. This plot illustrates the effect of impeller speed (RPM) on the mean residence time (τ) in a continuous stirred tank reactor (CSTR). The blue points represent observed experimental data, while the red curve shows a quadratic polynomial fit to the data. As the mixing speed increases, the mean residence time decreases, indicating enhanced mixing and reduced fluid retention time within the reactor.

From Figure 3(a), it is observed that higher mixing speeds (e.g., 490 RPM) result in a steeper initial slope, indicating a faster reduction in NaCl concentration over time. This behavior suggests that increased mixing enhances mass transfer and reduces concentration gradients within the reactor. Conversely, at lower mixing speeds (e.g., 50 RPM), the concentration decay is more gradual, leading to a broader RTD curve. This difference can be attributed to incomplete mixing at lower RPMs, where localized concentration pockets persist, prolonging the overall residence time distribution.

The second plot further supports this trend, demonstrating that as the impeller speed increases, the mean residence time decreases, indicating that particles exit the CSTR more quickly at higher mixing speeds. The quadratic polynomial fit suggests a nonlinear relationship, where a significant drop in residence time occurs between 250 and 490 RPM. The theoretical residence time was determined to be: 207.5 ± 0.5 seconds using the residence time definition by measuring the reactor volume and the volumetric flow rate[**6**]. At higher RPMs, the particles inside the reactor mix more frequently and more rapidly, better approximating ideal mixing conditions, leading to a more uniform distribution of reactants and minimizing dead zones and stagnant regions within the reactor. Consequently, the mean residence time at higher RPMs is closer to the theoretical residence time compared to lower RPMs. At lower RPMs, flow patterns deviate from the ideal mixing model, increasing fluid retention time, and broadening the RTD curve.

However, even at 490 RPM, there is still a deviation of approximately 5.8 percent between the experimental and theoretical residence times. This discrepancy may be attributed to the physical setup of the CSTR. One potential factor is that the actual reactor volume may be higher than the measured reactor volume due to pressure fluctuations at the effluent stream. Observations during RTD measurements showed that the liquid level in the CSTR was higher compared to when the reactor volume measurement was taken. It is expected from the experiment data that the mean residence time is higher than theoretical value because the actual volume is higher. Additionally, measurement uncertainties such as variations in conductivity probe response time or temperature inconsistencies affecting fluid viscosity may contribute to the observed deviation.

Furthermore, the quadratic trend suggests that beyond a certain mixing speed, further reductions in residence time become less significant as the system approaches near-ideal mixing conditions, where the residence time closely matches the theoretical value. This implies that once an optimal mixing speed is reached, increasing the impeller speed further may not provide substantial improvements in mixing efficiency. However, in practical applications, scaling up the reactor requires careful consideration of equipment limitations. Therefore, a relatively high but feasible mixing speed must be selected to balance efficient mixing with operational constraints. Based on these considerations, a mixing speed of 250 RPM was chosen for the CSTR setup, ensuring sufficient mixing while maintaining practical feasibility for scale-up.

4.3 Investigation of performance of CSTR reaction conversion and relatively optimal flowrate and temperature

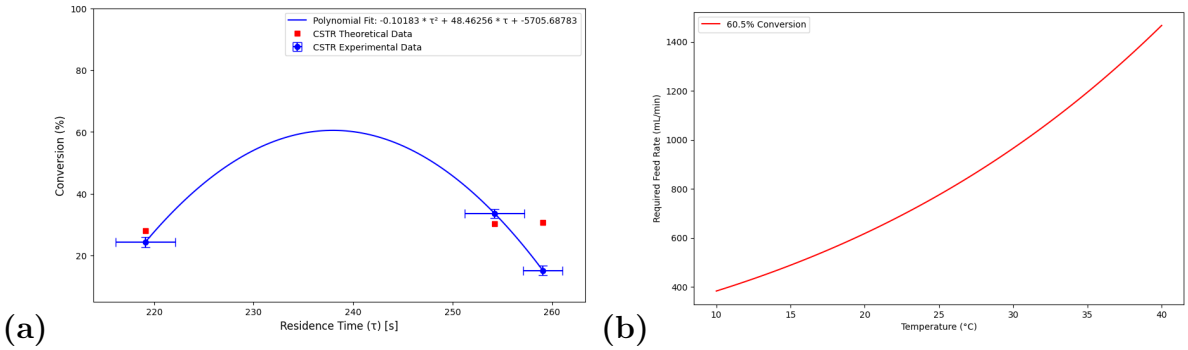

(a) (b)

Figure 4: **(a)** Relationship between residence time (τ) and conversion (%) in a Continuous Stirred Tank Reactor (CSTR). The experimental data (blue markers) and theoretical data (red squares) are compared, with horizontal error bars representing flow rate uncertainties and vertical error bars representing conversion uncertainties propagated in appendix B. A second-order polynomial fit (blue curve) is applied to the experimental data.(b) The plot illustrates the relationship between temperature (°C) and the required feed rate (mL/min) to achieve a maximally achievable 60.5% conversion. As the temperature increases, the required feed rate increases following an upward nonlinear trend, indicating higher temperature is necessary for maintaining the desired conversion rate at increased flow rates.

From Figure 4.a, it is observed that the conversion rate in the CSTR follows a nonlinear trend with respect to the residence time (τ), exhibiting an initial increase followed by a decline. A comparison between the experimental and theoretical data reveals noticeable deviations, with percent errors of approximately 12.2%, 15.5%, and 50.1% for the three residence times, respectively. Notably, the percent error increases significantly at higher residence times, indicating greater discrepancies between theoretical predictions and experimental observations. Under general expectations, at lower residence times (around 220 s), the conversion is relatively low because the reactants do not have sufficient time to undergo reaction before exiting the reactor. As the residence time increases, the reactants spend more time reacting, leading to a higher conversion. However, at higher residence times, the observed conversion is lower than expected. This phenomenon may be attributed to the back mixing effect[**8**], where low inlet and outlet flow rates lead to the accumulation of reaction products within the reactor. As more product builds up, it occupies significant space in the solution, preventing proper mixing of fresh reactants. This causes the dilution effect upon reactants, lowering the reactant concentrations in the vessel and reducing the overall reaction efficiency. Additionally, the presence of stagnant product-rich regions further limits mass transfer, decreasing the effective reaction rate and ultimately leading to a decline in conversion at higher residence times. The maximum conversion rate observed by the Department of Chemical Engineering at King Khalid University is 62.3%, which closely aligns with the maximum value predicted by our polynomial fit[**1**]. However, due to time constraints, the experiment failed to verify whether the maximum conversion occurs at the corresponding residence time. Therefore, future experiments are necessary to determine whether that specific residence time indeed yields the highest conversion.

Figure 4.b explores the relationship between flow rate and temperature required to achieve maximum conversion. As expected, at higher flow rates, a higher temperature is needed to maintain conversion since faster reactions lead to reduced reactant accumulation in the reactor. This plot serves as a valuable tool in establishing the manipulated variables essential for CSTR design. By analyzing this relationship, we can determine the optimal temperature set points needed for a given feed flow rate, ensuring efficient reactor performance.

5 Conclusions

In this study, the reaction kinetics of saponification of ethyl acetate with sodium hydroxide and reactor performance in a CSTR are analyzed. By identifying deviations from theoretical expectations due to dilution effects, back-mixing, and calibration inconsistencies, the study recognizes factors influencing the conversion efficiency. The activation energy determined is 30% than the reported value, suggesting experimental limitations. Future experiments could include trials to identify the feed rates at which maximum conversion is achieved. Additionally, future work should focus on improving flow calibration, refining temperature controls, and testing potential discrepancies caused by viscosity changes.

References

[1] Al Mesfer, M. K. Experimental Study of Batch Reactor Performance for Ethyl Acetate Saponification. *Int. J. Chem. React. Eng.* 2017, **2016**(0174). DOI: 10.1515/ijcre-2016-0174.

[2] Chada, J. Batch to Continuous Processing: Sodium Acetate from a Waste Stream of Ethyl Acetate. *ChE 180B: Chemical Engineering Laboratory*, Department of Chemical Engineering, University of California, Santa Barbara, Winter 2025.

[3] Fogler, H. S. *Elements of Chemical Reaction Engineering*, 5th ed.; Prentice Hall: 2016; Chapter 16: Residence Time Distributions of Chemical Reactors.

[4] Abu-Reesh, I. M. Optimal design for CSTRs in series using reversible Michaelis-Menten reactions. *Bioprocess Engineering* 1996, **15**, 257–264. DOI: `https://doi.org/10.1007/BF02391587`.

[5] Hu, C. Reactor design and selection for effective continuous manufacturing of pharmaceuticals. *J. Flow Chem.* 2021, **11**(3), 243-263. DOI: `10.1007/s41981-021-00164-3`. PMID: 34026279; PMCID: PMC8130218.

[6] Author(s) Unknown. *Chemical Reaction Engineering Handbook*; Gulf Professional Publishing: 1997. Available online: `https://www.sciencedirect.com/science/article/abs/pii/B9780884154815500103` (accessed February 4, 2025).

[7] Gawdzik, B.; Matlengiewicz, M. Effect of Viscosity on the Kinetics of Living Polymerization. *J. Appl. Polym. Sci.* 2020, **137**(28), 48857. DOI: `10.1002/app.48857`.

[8] Gültekin, S.; Kalbekov, A. Effect of back mixing on the performance of tubular-flow reactors. *Int. J. Dev. Res.* 2017, **7**, 10432. Available online: `https://www.journalijdr.com/effect-back-mixing-performance-tubular-flow-reactors` (accessed February 5, 2025).

A Raw Data

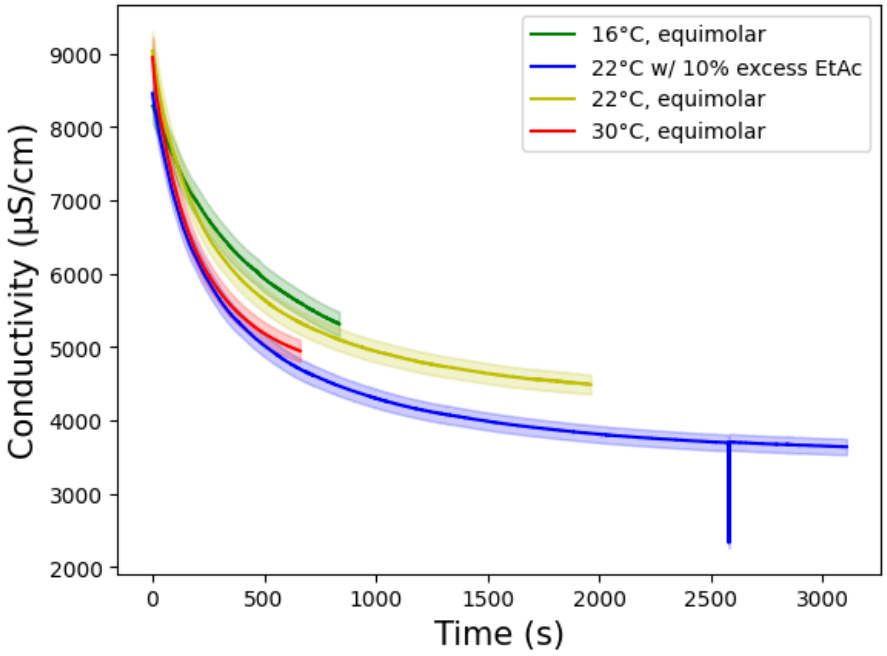

Figure A1: Batch reactor's experimental data with different reaction temperature. The conductivity decrease over time as NaOH, the reactant with higher conductivity, gradually converting into NaAc, the product with lower conductivity.

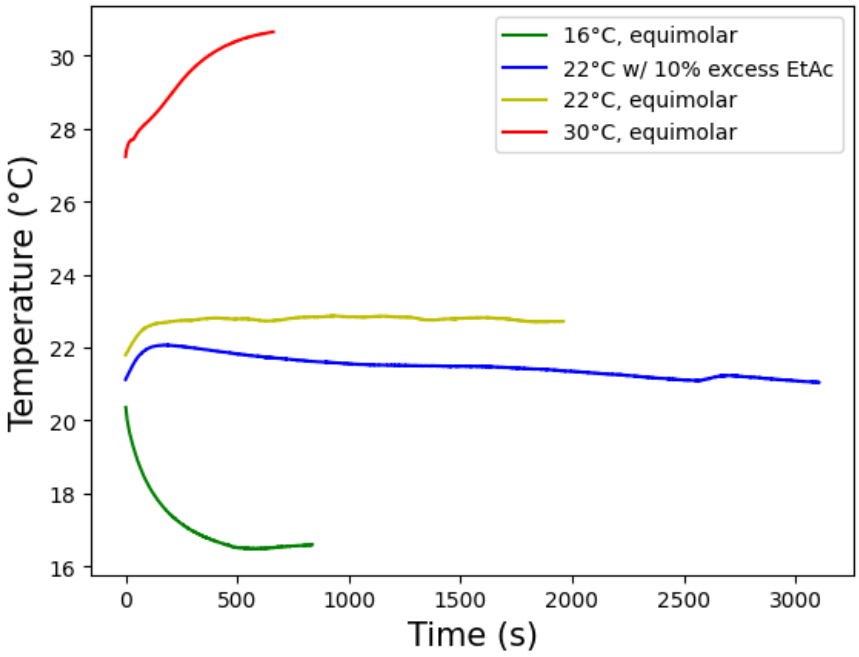

Figure A2: Actual temperature inside the reactor when water bath was set at 16, 22, 30 °C. Since the reaction is exothermic, the temperature inside the reactor varies as the concentration of reactants and products changed.

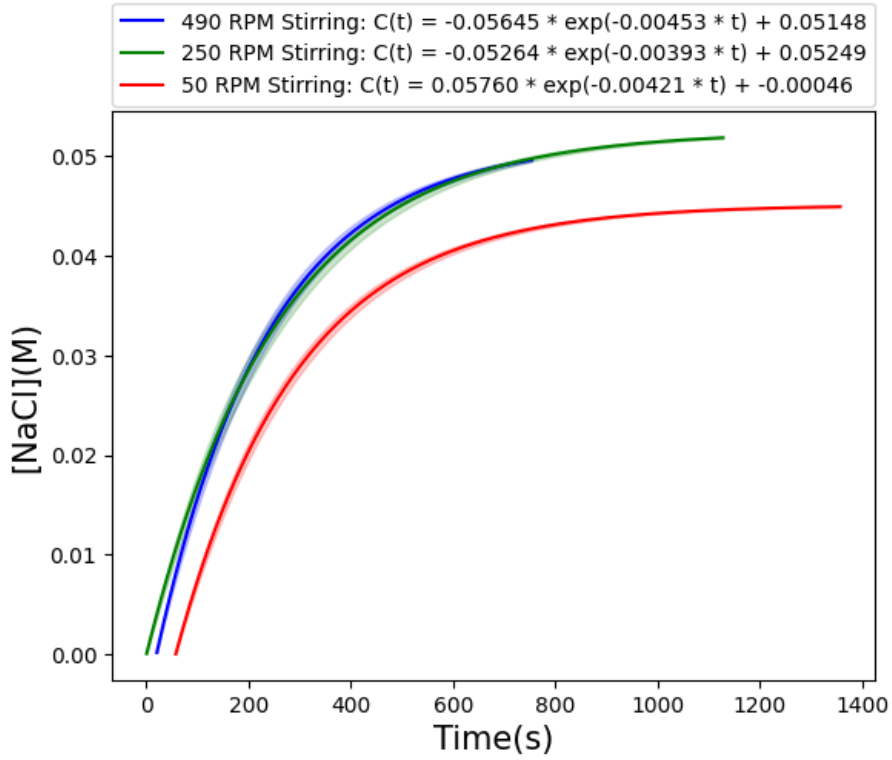

Figure A3: Results of the positive step test for RTD analysis to determine τ. The feed rate was maintained at 226.17 $\pm$ 0.005 mL/min, while the stirring speed was varied to study its effect on the reaction rate and mixing dynamics.

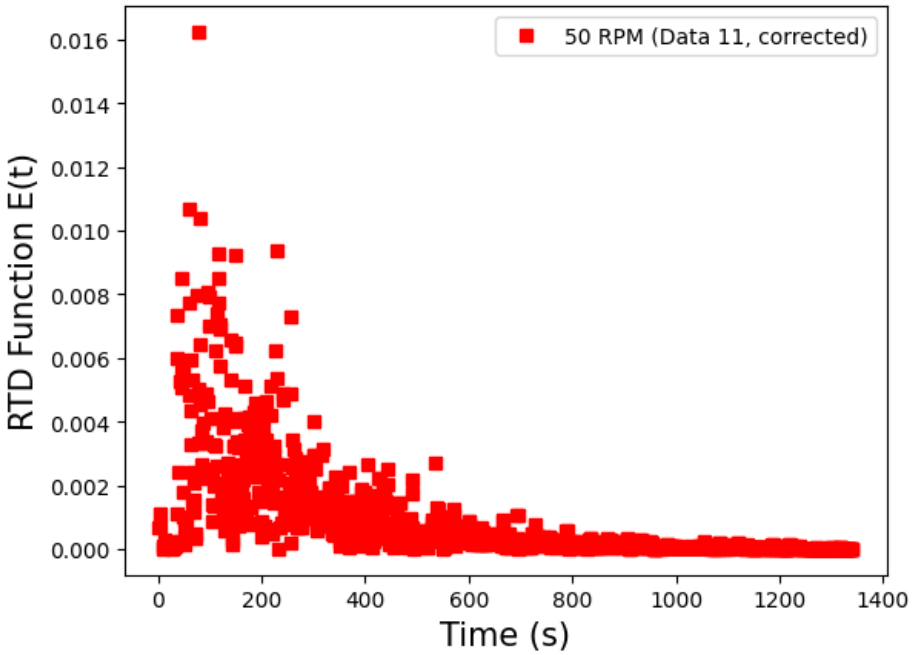

Figure A4: Residence Time Distribution (RTD) Function for 50 RPM (Filtered). This plot represents the RTD function $E(t)$ over time for the CSTR operating at 50 RPM.

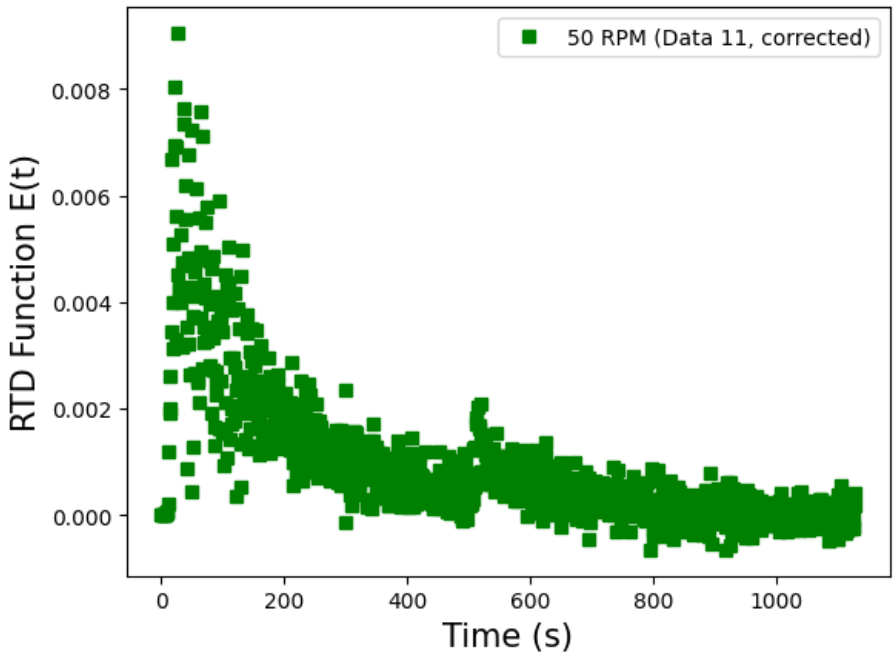

Figure A5: Residence Time Distribution (RTD) Function for 50 RPM (Filtered). This plot represents the RTD function $E(t)$ over time for the CSTR operating at 250 RPM.

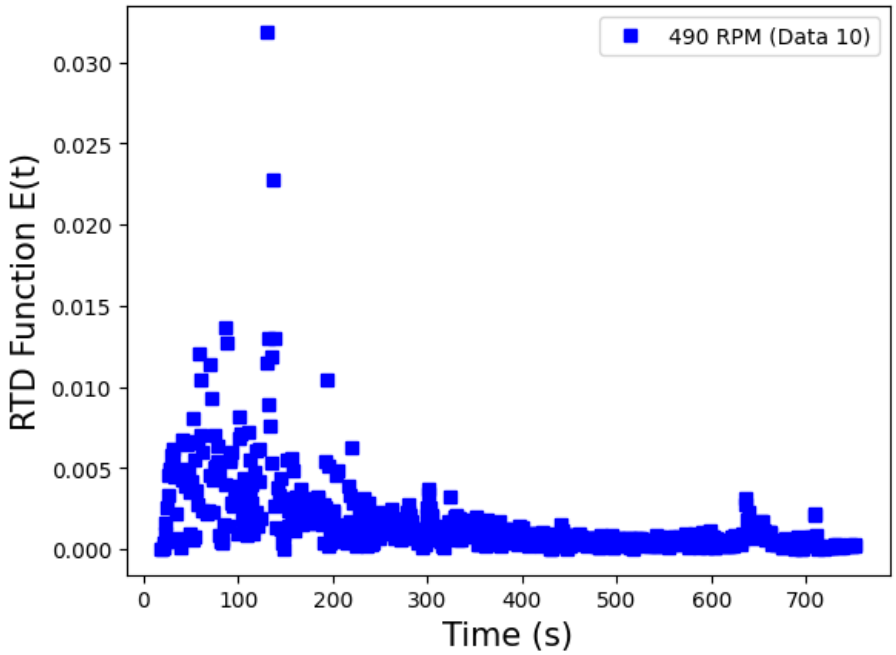

Figure A6: Residence Time Distribution (RTD) Function for 50 RPM (Filtered). This plot represents the RTD function $E(t)$ over time for the CSTR operating at 490 RPM.

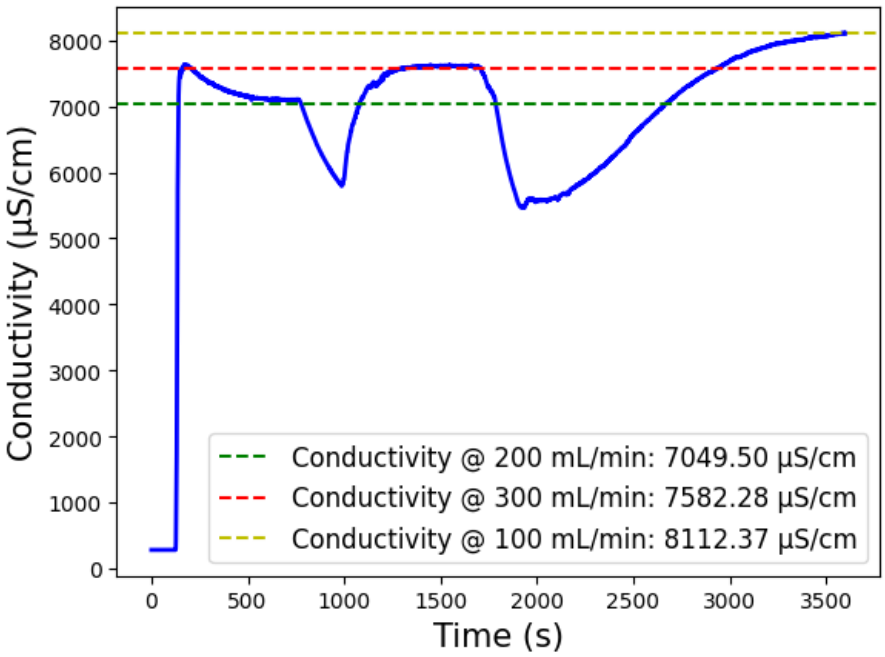

Figure A7: Experimental CSTR data collected at a constant stirring rate of 250 rpm, with varying flow rates. The stabilized conductivity values were used to calculate the product concentration, which was then used to determine the conversion.

B Sample Calculations

B.1 Determination of Reactant Concentration from Conductivity

The concentration of NaOH is determined using the relationship:

$$[\text{NaOH}] = [\text{NaOH}]_0 \frac{\Lambda - \Lambda_\infty}{\Lambda_0 - \Lambda_\infty} \tag{B.1}$$

Given:

$$[\text{NaOH}]_0 = 0.05 \text{ M}$$
$$\Lambda_0 = 8500 \text{ µS/cm}, \quad \Lambda_\infty = 3000 \text{ µS/cm}$$

At a given conductivity $\Lambda = 6000$ µS/cm:

$$[\text{NaOH}] = 0.05 \times \frac{6000 - 3000}{8500 - 3000} \tag{B.2}$$

$$[\text{NaOH}] = 0.0273 \text{ M}$$

B.2 Determination of Rate Constant k

The second-order rate law is:

$$\frac{1}{C_A} - \frac{1}{C_{A0}} = kt \tag{B.3}$$

Using experimental data:

$$C_{A0} = 0.05 \text{ M}$$
$$C_A = 0.014 \text{ M at } t = 661 \text{ s}$$

$$k = \frac{\frac{1}{0.014} - \frac{1}{0.05}}{661} \tag{B.4}$$
$$k = 0.0045 \text{ L mol}^{-1}\text{s}^{-1}$$

B.3 Determination of Reactant Concentration from Conductivity

The concentration of NaOH is determined using the relationship:

$$[\text{NaOH}] = [\text{NaOH}]_0 \frac{\Lambda - \Lambda_\infty}{\Lambda_0 - \Lambda_\infty} \tag{B.5}$$

Given:

$$[\text{NaOH}]_0 = 0.05 \text{ M}$$
$$\Lambda_0 = 8500 \text{ µS/cm}, \quad \Lambda_\infty = 3000 \text{ µS/cm}$$

For a measured conductivity $\Lambda = 6000$ µS/cm:

$$[\text{NaOH}] = 0.05 \times \frac{6000 - 3000}{8500 - 3000} \tag{B.6}$$

$$[\text{NaOH}] = 0.0273 \text{ M}$$

B.4 Determination of Rate Constant k Using Linear Fitting

For a second-order reaction, the rate law is:

$$\frac{1}{C_A} - \frac{1}{C_{A0}} = kt \tag{B.7}$$

Rearranging into a linear form:

$$\frac{1}{C_A} = kt + \frac{1}{C_{A0}} \tag{B.8}$$

which is of the form $y = mx + b$, where: - $y = \frac{1}{C_A}$, - $x = t$, - $m = k$ (slope), - $b = \frac{1}{C_{A0}}$.

To determine k, experimental data of C_A vs. time is collected, and a plot of $1/C_A$ vs. time is constructed.

By performing a linear fit, the slope and the error of the line is determined as:

$$k = 0.0525 \pm 0.0003 \text{ L mol}^{-1}\text{s}^{-1} \quad (\text{at } 25^\circ\text{C}) \tag{B.9}$$

B.5 Arrhenius Plot for Determining A and E_a

The Arrhenius equation is:

$$k = Ae^{-E_a/RT} \tag{B.10}$$

Taking the natural logarithm:

$$\ln k = \ln A - \frac{E_a}{R} \cdot \frac{1}{T} \tag{B.11}$$

Using experimental values of k obtained from linear fitting at different temperatures:

Temperature (K)	**Rate Constant, k (L mol^{-1}s^{-1})**
289	0.0427 ± 0.0002
295	0.0525 ± 0.0003
303	0.0800 ± 0.0003

Table 1: Experimental Values of k at Different Temperatures

The linear fit is shown in C.3. From the linear fit, the slope and the error of the line is determined to be -3.966 ± 0.5:

$$E_a = -\text{slope} \times R \tag{B.12}$$

$$E_a = 33.0 \pm 1.2 \text{ kJ/mol}$$

Error in Activation Energy E_a

The error propagation equation for E_a is:

$$\sigma_{E_a} = \left|\frac{\partial E_a}{\partial k_1}\right| \sigma_{k_1} + \left|\frac{\partial E_a}{\partial k_2}\right| \sigma_{k_2} \tag{B.13}$$

Assuming $\sigma_{k_1} = \pm 0.0002$ and $\sigma_{k_2} = \pm 0.0003$:

$$\sigma_{E_a} = \pm 1.2 \text{ kJ/mol}$$

The **pre-exponential factor** A is determined from the intercept:

$$A = ke^{E_a/RT} \tag{B.14}$$

Using $k = 0.0023$ at $T = 288$ K:

$$A = 0.0023e^{32700/(8.314\times 288)} \tag{B.15}$$

$$A = 3.80 \times 10^4 \text{ L mol}^{-1}\text{s}^{-1}$$

Error Propagation for Pre-Exponential Factor A

The Arrhenius equation is:

$$k = Ae^{-E_a/RT} \tag{B.16}$$

Solving for A:

$$A = ke^{E_a/RT} \tag{B.17}$$

Using error propagation, the uncertainty in A is:

$$\sigma_A = A\sqrt{\left(\frac{\sigma_k}{k}\right)^2 + \left(\frac{\sigma_{E_a}}{RT}\right)^2} \tag{B.18}$$

Substituting values:

$$\begin{aligned} k &= 0.0023 \text{ L mol}^{-1}\text{s}^{-1}, \quad A = 3.45 \times 10^4 \text{ L mol}^{-1}\text{s}^{-1}, \\ E_a &= 32.7 \text{ kJ/mol}, \quad R = 8.314 \text{ J/(mol K)}, \quad T = 288 \text{ K} \\ \sigma_k &= \pm 0.0002 \text{ L mol}^{-1}\text{s}^{-1}, \quad \sigma_{E_a} = \pm 1.2 \text{ kJ/mol} \end{aligned}$$

$$\sigma_A = (3.45 \times 10^4)\sqrt{\left(\frac{0.0002}{0.0023}\right)^2 + \left(\frac{1.2 \times 10^3}{(8.314 \times 288)}\right)^2} \tag{B.19}$$

$$\sigma_A = (3.45 \times 10^4)(0.1002) \tag{B.20}$$

$$\sigma_A = 3450 \text{ L mol}^{-1}\text{s}^{-1} \tag{B.21}$$

Thus, the final result is:

$$A = (3.45 \pm 0.35) \times 10^4 \text{ L mol}^{-1}\text{s}^{-1} \tag{B.22}$$

B.6 Batch Reactor Design Equation Solution

For a batch reactor, the design equation is:

$$\frac{dC_A}{dt} = -kC_AC_B \tag{B.23}$$

Using equal initial concentrations, $C_A = C_B$:

$$\frac{1}{C_A} - \frac{1}{C_{A0}} = kt \tag{B.24}$$

Solving for conversion at $t = 200$ s:

$$X = 1 - \frac{C_A}{C_{A0}} = 1 - \frac{1}{1 + ktC_{A0}} \tag{B.25}$$

Substituting $k = 0.0071$ and $C_{A0} = 0.05$ M:

$$X = 0.415$$

Error Propagation for Conversion

$$\sigma_X = \sqrt{\left(\frac{\partial X}{\partial C_A}\sigma_{C_A}\right)^2 + \left(\frac{\partial X}{\partial C_{A0}}\sigma_{C_{A0}}\right)^2} \tag{B.26}$$

Substituting experimental uncertainties:

$$\sigma_X = \pm 0.015$$

B.7 Residence Time Distribution (RTD) from Step Test

The RTD function $E(t)$ is:

$$E(t) = \frac{dF(t)}{dt} \tag{B.27}$$

where:

$$F(t) = \frac{C(t)}{C_0} \tag{B.28}$$

At steady state, the mean residence time is:

$$\tau = \int_0^\infty tE(t)dt \tag{B.29}$$

Using experimental RTD data, $\tau = 254$ s when mixing speed is 250 rpm.

Error Propagation in Residence Time Calculation

The residence time (τ) is determined from the RTD function as:

$$\tau = \int_0^\infty tE(t)dt \tag{B.30}$$

where $E(t)$ is the **RTD function**, and $F(t)$ is the cumulative distribution function:

$$E(t) = \frac{dF(t)}{dt}, \quad F(t) = \frac{C(t)}{C_0} \tag{B.31}$$

Since the experimental RTD data is discrete, τ is estimated numerically as:

$$\tau = \sum_i t_i E(t_i) \Delta t \tag{B.32}$$

where: - t_i are discrete time points, - $E(t_i)$ are the corresponding RTD values, - Δt is the time interval between measurements.

Error Propagation in τ

To determine the uncertainty in residence time, we apply the **error propagation formula**:

$$\sigma_\tau = \sqrt{\sum_i \left(\frac{\partial \tau}{\partial E(t_i)} \sigma_{E(t_i)} \right)^2 + \sum_i \left(\frac{\partial \tau}{\partial t_i} \sigma_{t_i} \right)^2} \tag{B.33}$$

Since τ is a weighted sum of $t_i E(t_i)$, the partial derivatives are:

$$\frac{\partial \tau}{\partial E(t_i)} = t_i \Delta t, \quad \frac{\partial \tau}{\partial t_i} = E(t_i) \Delta t \tag{B.34}$$

Thus, the uncertainty in τ can be computed as:

$$\sigma_\tau = \sqrt{\sum_i (t_i \Delta t \sigma_{E(t_i)})^2 + \sum_i (E(t_i) \Delta t \sigma_{t_i})^2} \tag{B.35}$$

Using experimental RTD data, the measured residence time at 250 rpm is:

$$\tau = 254 \pm 5 \text{ s} \tag{B.36}$$

where the error σ_τ is estimated based on variations in RTD measurements.

B.8 CSTR Design Equation

The steady-state CSTR equation is:

$$C_{A0} - C_A + \tau(-r_A) = 0 \tag{B.37}$$

Using $r_A = kC_A^2$:

$$C_A = \frac{C_{A0}}{1 + k\tau C_{A0}} \tag{B.38}$$

For $C_{A0} = 0.05$ M, $\tau = 254$ s:

$$C_A = 0.0176 \text{ M}$$

Conversion:

$$X = 1 - \frac{C_A}{C_{A0}} = 0.648$$

Error Propagation in CSTR Design Equation

The CSTR steady-state concentration is given by:

$$C_A = \frac{C_{A0}}{1 + k\tau C_{A0}} \tag{B.39}$$

where C_A is the outlet concentration, C_{A0} is the inlet concentration, k is the rate constant, and τ is the residence time.

Using error propagation, the uncertainty in C_A is calculated as:

$$\sigma_{C_A} = \sqrt{\left(\frac{\partial C_A}{\partial C_{A0}}\sigma_{C_{A0}}\right)^2 + \left(\frac{\partial C_A}{\partial k}\sigma_k\right)^2 + \left(\frac{\partial C_A}{\partial \tau}\sigma_\tau\right)^2} \tag{B.40}$$

The partial derivatives are:

$$\frac{\partial C_A}{\partial C_{A0}} = \frac{1}{(1 + k\tau C_{A0})^2} \tag{B.41}$$

$$\frac{\partial C_A}{\partial k} = -\frac{C_{A0}\tau}{(1 + k\tau C_{A0})^2} \tag{B.42}$$

$$\frac{\partial C_A}{\partial \tau} = -\frac{kC_{A0}}{(1 + k\tau C_{A0})^2} \tag{B.43}$$

Substituting values:

$$C_{A0} = 0.05 \text{ M}, \quad k = 0.0045 \text{ L mol}^{-1}\text{s}^{-1}, \quad \tau = 254 \text{ s}$$
$$\sigma_{C_{A0}} = \pm 0.001 \text{ M}, \quad \sigma_k = \pm 0.0002 \text{ L mol}^{-1}\text{s}^{-1}, \quad \sigma_\tau = \pm 5 \text{ s}$$

$$C_A = \frac{0.05}{1 + (0.0045)(254)(0.05)} \tag{B.44}$$
$$C_A = 0.0176 \text{ M}$$

Computing σ_{C_A}:

$$\sigma_{C_A} = \pm 0.0008 \text{ M} \tag{B.45}$$

Thus, the final result is:

$$C_A = 0.0176 \pm 0.0008 \text{ M} \tag{B.46}$$